Neutron Stress Imaging of Drawn Copper Tube: Comparison with Finite-Element Model

T. PIRLING, A. CARRADÒ, S. BRÜCK, and H. PALKOWSKI

Seamless tubes are used for various mechanical applications, often produced by several cold drawing steps to reach the required dimensions. The first process step, for example, extrusion or rolling, typically results in ovality and eccentricity of the tube caused by nonsymmetric material flow and being present during the cold drawing process, *i.e.*, no homogeneous deformation. Because of this nonsymmetrical deformation, and deviations over the length of the tube caused by moving tools, this process step generates inhomogeneous residual stresses. To understand the interconnection between geometrical changes in the tubes and the resulting residual stresses, the residual strain distribution in a copper tube was measured by neutron diffraction. The aim of this study is to evaluate residual stresses generated during cold drawing of copper tubes. This research comprises experimental measurements and numerical analysis. An industrially produced copper tube was cold drawn, and the profile of residual strain over circumference and across wall thickness was measured by neutron diffraction. In parallel, a three-dimensional finite-element model (FEM) was developed to calculate the residual macrostress state generated by the forming process. Good agreement between experimental results and numerical computations was obtained.

I. INTRODUCTION

COLD drawn seamless tubes are used for many applications, *e.g.*, for plumbing, in heating systems, oil and gas pipes, drinking water systems, transport of medical and industrial gases, evaporators, as well as intermediate products for hydroforming and various mechanical applications.[1]

For industrial production of seamless tubes, the first forming step often is piercing of the billet, for example, by extrusion. Due to vibrations of the mandrel, tolerances in positioning of the die and billet, as well as potential temperature differences within the billet, this step inherently results in variations of thickness over length, eccentricity, and ovality. These geometrical irregularities can be found downstream through the complete process route.

The eccentricity E of the tube is defined as the deviation of the wall thickness from an average value (Figure 1): $E = t_{max} - t_{min}/t_{ave} \times 100$ pct with t_{max} and

T. PIRLING, Instrument Scientist, is with the Institut Laue-Langevin, BP 156 - 38042 Grenoble Cedex 9, France. A. CARRADÒ, Associate Professor of University of Strasbourg, is with the Institut de Physique et Chimie des Matériaux de Strasbourg, 67034 Strasbourg Cedex 2, France. Contact e-mail: adele.carrado@ipcms.u-strasbg.fr S. BRÜCK, Postdoctoral Student, and H. PALKOWSKI, Chair of Metal Forming, are with the Institute of Metallurgy, Clausthal University of Technology, 38678 Clausthal-Zellerfeld, Germany.
This article is based on a presentation given in the symposium entitled "Neutron and X-Ray Studies for Probing Materials Behavior," which occurred during the TMS Spring Meeting in New Orleans, LA, March 9–13, 2008, under the auspices of the National Science Foundation, TMS, the TMS Structural Materials Division, and the TMS Advanced Characterization, Testing, and Simulation Committee.
Article published online September 16, 2008

t_{min} the maxima and minima wall thicknesses, respectively, and t_{ave} the average wall thickness. For industrial tubes, the eccentricity lays typically around 5 to 10 pct for steel and about 5 pct for aluminum grades.[2,3]

The ovality O is the deviation of the external cross section from a perfect circular shape: $O = d_{max} - d_{min}/d_{ave} \times 100$ pct, with d_{max} and d_{min} the maximum and minimum external diameters, respectively, and d_{ave} the average external diameter. Industrial tubes typically exhibit up to 1 pct ovality for carbon steel tubes and up to 3 pct for copper tubes.[4,5]

In order to achieve the final diameter and wall thickness, the extruded tubes are reduced successively in additional cold drawing steps with or without using a plug (Figures 2(a) and (b)). Different kinds of plugs can be used to influence the wall thickness. The method is well known and described in books about metal forming processes, such as in References 6 through 8. Figure 2(a) shows an example of a running plug, Figure 2(b) shows the geometrical data of a die, where γ is the so-called drawing angle and L the length of the drawing tool. The dimensions used in this investigation are listed in Table I.

During subsequent drawing steps, the tube undergoes plastic deformation, generating residual stresses on unloading. Moreover, eccentricity of semifinished products influences the material flow over the circumference, generating a complex residual stress pattern[9,10] that can affect the mechanical and fatigue behavior of the tube. Because of the inhomogeneous plastic deformation through the volume, metal forming results in residual stresses within the whole cross section of the material.[11] Prestudies showed a periodicity in thickness and hardness deviation, which are discussed in Reference
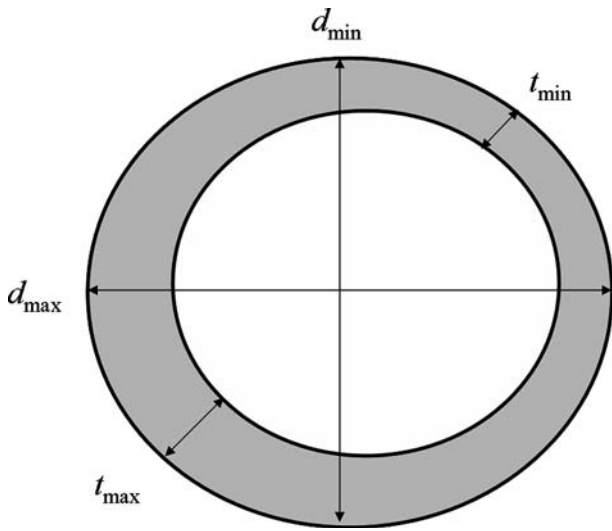
Fig. 1—Schematic cross section of the tube emphasizing ovality and eccentricity.
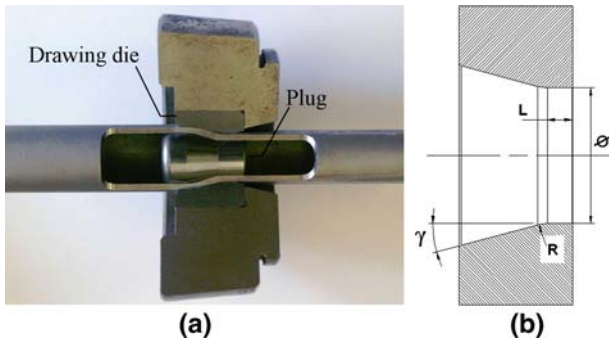

Fig. 2—(a) Photograph of drawing tool and (b) schematic cross section of a drawing die.

Table I. List of Die Parameters: γ—Drawing Angle; R—Radius; L—Length; and Ø—Inner Diameter (Figure 2(b))

Number	γ (Deg)	R (mm)	L (mm)	Ø (mm)
35	15	12	10	45.24

12. Local inspection of residual stresses by a strain gage method showed clearly their nonconstant behavior around the circumference and over length.[13] Residual stresses can also play an important role on crack formation and corrosion.[14]

Knowing that residual micro-stresses of the second and third kind occur in such, on macroscopic scale homogeneous, cold-forming processes, macroscopic deformation gradients cause first-order residual stresses. Thus, it is possible to influence their distribution in both amount and sign by variation of the tool geometry and other parameters of the forming process.[15] Whereas most investigations assume the ideal rotationally symmetric case, the behavior of eccentric tubes, which are the standard among most industrially manufactured ones, is still unknown. Thus, it is necessary to investigate these nonideal tubes for a better understanding of the development of those residual stresses and their relation to eccentricity in order to reach smaller geometrical tolerances.[16]

Whereas compressive residual stresses at the surface of the tube can be advantageous and are sometimes intentionally introduced, for example, by shot peening, tensile residual stresses are often harmful and tend to decrease the formability and favor the appearance of cracks. By minimizing harmful residual stresses, the necessity of heat treatment or straightening steps can be avoided. This could considerably reduce the cost of the production process.

In the present article, the mechanical behavior (thickness and residual stresses) of a copper tube specimen, which is representative for those used for heat exchangers, is described. Neutron (diffraction) strain imaging was used to determine residual stresses. The aim of this investigation is to quantify the change of residual stresses over the circumference of a drawn copper tube and to find correlations with mechanical and geometrical properties.

II. FINITE-ELEMENT MODELING

A three-dimensional finite-element model (FEM) was developed to study the residual macrostress state generated by the forming process. For the tools, die and plug rigid elements were chosen to reduce the calculation time significantly with small loss of accuracy in the results. The die is fixed in all degrees of freedom; the plug can only move in the radial direction. This degree of freedom is necessary due to the unknown material flow in the deformation zone without plug contact.

In order to take bending effects into account, the length chosen for the tube model was 60 mm, although the deformation zone is much shorter. These effects influence stresses in the tube parts before they reach the deformation zone. Additionally, it is necessary for computation to keep a minimum of drawing length in order to obtain realistic constant boundary conditions in the deformation zone. Because of its symmetry in thickness deviation, the tube model calculates only one half of the tube. The start of the tube is only moved in the drawing direction and not fixed in any other direction.

Explicit analysis followed by an implicit calculation step was chosen. One advantage of the explicit procedure over the implicit one is the greater ease with which it resolves complicated contact problems such as movements of the plug and tube in the radial direction. In addition, as models become very large, the explicit procedure requires less system resources than the implicit procedure.

After the tube leaves the drawing tool, a stress wave evolves, because of fast changing external load, which adds up to residual stresses. This can be compared with the spring-back problem in sheet forming.

While an explicit approach is well suited for the drawing simulations, stress waves pose some specific difficulties. The main problem related to performing

spring-back simulations within explicit calculations is to get the time constant right, which is required to obtain a steady-state solution. In general, the external load must be removed smoothly and a damping factor must be introduced to make the solution time sensible. Fortunately, the close relationship between explicit and implicit calculations allows a much more efficient approach.

Tube modeling takes into account the mechanical material behavior with a classic plasticity model, which uses the Mises yield surfaces with associated plastic flow. As a first step of simulation, the Mises yield surface was chosen to define isotropic yielding. It is defined by giving the value of the uniaxial yield stress as a function of uniaxial equivalent plastic strain (PEEQ).

The PEEQ is defined using the following equation:

$$\bar{\varepsilon}^{pl}\big|_0 + \int_0^t \dot{\bar{\varepsilon}}^{pl} dt$$

where $\bar{\varepsilon}^{pl}\big|_0$ is the initial equivalent plastic strain and $\dot{\bar{\varepsilon}}^{pl}$ depends on the material model. For metals such as steel or copper, considering the approximation of von Mises, the plasticity is defined as

$$\dot{\bar{\varepsilon}}^{pl} = \sqrt{\frac{2}{3}\dot{\varepsilon}^{pl} : \dot{\varepsilon}^{pl}}$$

The material properties of copper, derived from tensile testing were Young's modulus (E) 130 GPa and Poisson's ratio (ν) 0.34.

The flow curve $f(\varphi)$, with deformation φ, is defined using the equation

$$f(\varphi) = 56.1 + 1847.8\cdot\varphi - 5178.2\cdot\varphi^2 + 8262.3\cdot\varphi^3$$
$$- 6632\cdot\varphi^4 + 2061.8\cdot\varphi^5$$

This equation is a polynomial interpolation of experimental data of the same copper alloy, obtained at the University of Clausthal.[24]

The thermal behavior is not taken into account in this model, because temperature variations by this deformation step are relatively small. Plastic strain was considered incompressible and eight-node linear brick elements with reduced integration were chosen. Different mass scaling factors and element sizes were investigated, to obtain a good compromise between calculation time and accuracy.

The contact between the tube and the tools was modeled with a Coulomb friction factor of 0.05, which is a common practice value. Stresses, strains, and forces for the drawing process as well as final residual stresses after drawing were calculated. Figure 3 shows the
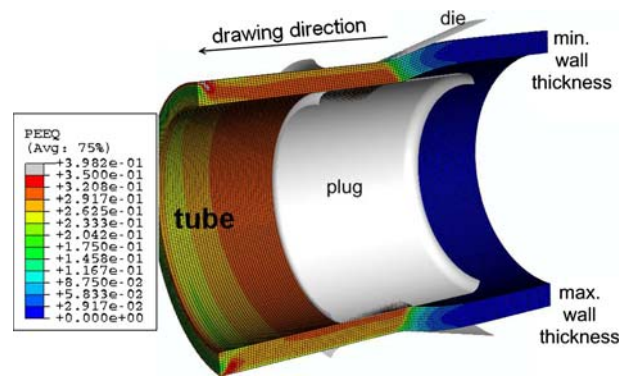

Fig. 3—Three-dimensional FEM of the tube with contour plot of equivalent plastic strain.

contour plot of the FEM of the tube including the tools as a rigid body during the drawing process. The colors for the tube elements represent the equivalent plastic strain (blue: min = 0; and gray: max = 0.39), and they show the highest differences between the minimum and the maximum wall thicknesses because of different material flows. This causes as well different residual stresses in these locations.

III. SAMPLE PREPARATION

A raw tube (DIN SF-Cu: 99.90 pct min Cu, and 0.015 to 0.040 pct P) was produced by extrusion, drawn twice in a cold-drawing process and stress annealed before being drawn to its final dimension. The processing data are shown in Table II.

The characteristics of the investigated sample are given in Table III. A 500-mm-long section of the tube has been used for investigations. Because cutting modifies the stress pattern, the strain measurements were performed 100 mm away from the cut, far enough to be unaffected, as verified in pretests.

The degree of deformation in diameter (φ_d) and wall thickness (φ_t) is defined as $\varphi_d = \ln\left(d_1 - t_1/d_0 - t_0\right)$ and $\varphi_t = \ln\left(t_1/t_0\right)$, with the subscripts 0 and 1 referring to

Table II. Processing Data of the SF-Cu Tube

Type of Parameters	$\langle d \rangle$ (mm)	$\langle t \rangle$ (mm)	φ_d	φ_t	Q
Extrusion	85	5.0			
Drawing	70	4.5	−0.19	−0.20	1.05
Drawing	50	4.0	−0.34	−0.35	1.03
Annealing 680 °C, 6.5 h, continuous furnace.					

Table III. Forming Parameters Used for Drawn SF-Cu Tubes

Plug Ø (mm)	Deformation $\varphi_d + \varphi_t$	Die (Number)	Outer Ø, Tube (mm)		Average Thickness (mm)		ΔThickness (mm)		Ovality O (Pct)	Eccentricity E (Pct)	
			Before	After	Before	After	Before	After		Before	After
38.00	0.2	35	50.0	45.24	4.0	3.62	0.4	0.33	<0.05	5.0	4.5

the tube before and after drawing, respectively. The deformation ratio $Q = \varphi_t/\varphi_d$ is an important parameter for tube drawing. The value of Q describes the main direction of plastic flow.[8] A high Q value means that the deformation follows mainly from the reduction of the wall thickness. Therefore, a small value indicates that the elongation of the tube results from the reduction of the diameter.

IV. NEUTRON MEASUREMENTS

From all nondestructive residual stress techniques, neutron diffraction was chosen because it is well adapted to evaluate stresses in bulk material.[17] The experiments presented in this article were performed on the strain imager for engineering applications SALSA at the Institut Laue-Langevin (Grenoble, France). The instrument was chosen, because it is equipped with two radial focusing collimators, which provide a very low surface error[18] and are therefore well suited for measurements in thin-walled samples.

The beam width was 0.6-mm full width half maximum (FWHM), which leads to a lateral resolution of about 0.8 mm in the scan direction. Through-thickness scans with 0.5-mm step size were performed in order to capture the expected stress gradients. These measurements were done in three orthogonal orientations, assuming the principal axes correspond to the sample symmetry, axial, radial, and hoop, as sketched out in Figure 4.

SF-Cu has a face-centered-cubic structure with space group $Fm3m$ and lattice parameter $a_0 = 0.36148$ nm. Because SALSA is a monochromatic strain imager, the family of planes {311} was used for stress determination at a wavelength of $\lambda = 0.165$ nm. This brings the diffraction angles to $2\theta \sim 98$ deg, providing an equally shaped gage volume for both measuring geometries, reflection and transmission.

Complete through-thickness scans have been performed at four locations, separated by 90 deg, starting from the reference line, as marked in Figure 4, which is defined as position 0 deg. The maximum wall thickness t_{max} lies at position 90 deg and the thinnest t_{min} at position 270 deg.

Fig. 4—Sample geometry for the measurement of triaxial strains on the SALSA strain imager.

Table IV. Experimental Parameters and Conditions for Measurements on the SF-Cu Tube

Equipment	SALSA (ILL)
Method	triaxial
Monochromator	double focusing, bent Si crystals
Wavelength (nm)	0.165
Detector	two-dimensional position sensitive microstrip detector
Beam shaping optics	radial focusing collimators, vertical slit
Gauge volume (mm³)	$0.6 \times 0.6 \times 5$ or 3
Diffracting planes	{311}
Acquisition time (min)	10
α angles (deg)	0, 90, 180, 270
E_{macro} (GPa)	124 (literature)
v_{macro}	0.343 (literature)

Table IV summarizes the experimental parameters as well as the elastic constants used for stress determination. The reference lattice parameter d_0 has been determined from stress balancing.

V. RESULTS AND DISCUSSION

The results of neutron measurements show a clear development of stress over thickness for all stress directions and the four chosen angular positions. The stress level at the outside of the tube is in tension and changing to a compressive state at the inner side ("0" position in Figure 5). The radial component in all cases is roughly zero, as can be expected, because of the quite thin shell of the tube. This may differ for thick-walled ones. The axial component shows the largest level of stress, though relatively the hoop stress is only slightly smaller, which is in agreement with the results from Reference 20.

There is not a significant difference between the stress evolution of the thinnest (270 deg) and the thickest (90 deg) parts of the tube. Data vary only by about 20 to 30 MPa with a statistical uncertainty of ±12 MPa. However, a significant effect is the different behavior at the outer side of the tube at 90 deg, where there is a clear plateau visible, compared to the other ones. This is in good agreement with the FEM, which corresponds to other measurements done previously such as those in References 20 through 22. The other ones show more or less a linear increase from the inside to the outside of the tube.

The stress development in this industrially produced tube does not correlate with differences in measured and calculated thicknesses (Figure 5), where, clearly, a different flow can be seen. From these results, it seems that eccentricity has only minor influence on the stress distribution. In Reference 23, it has been shown that the industrial produced tubes (our pretubes) show changing eccentricity in the drawing direction over short distances, which of course influences movements of plug and tube and therefore the material flow. Other important factors could be the movement of the tube before and after the die and chattering of the plug. However, more measurements with systematically varied process
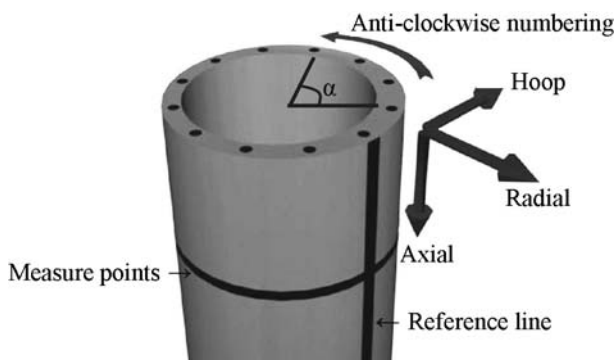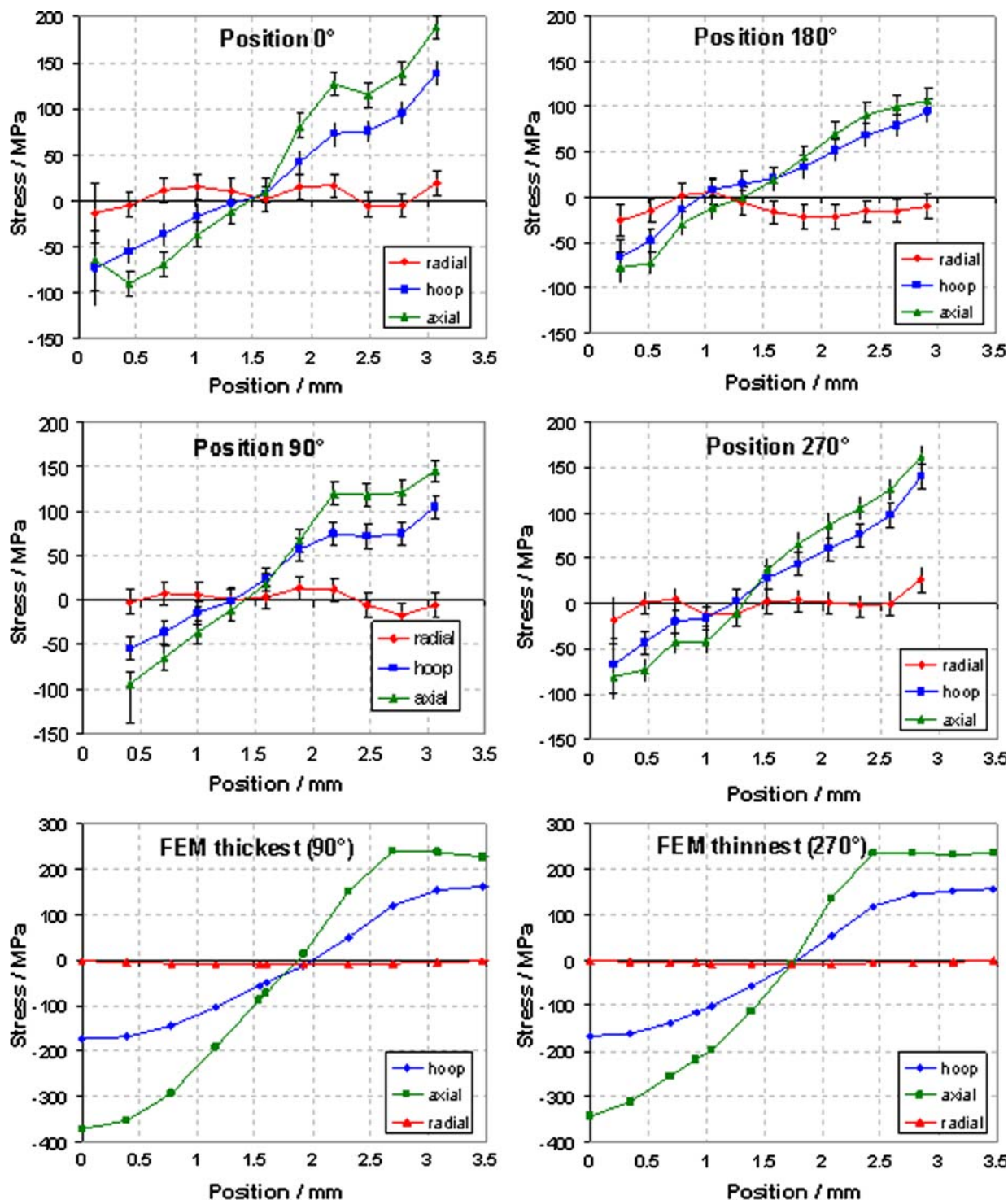
Fig. 5—Residual stresses determined at the four locations around the circumference of the tube, as explained in the text. At the bottom: FEM calculations for the thinnest (270 deg) and thickest parts of the wall (90 deg).

parameters will follow in order to evaluate as well the influence of other processing parameters, such as drawing without plug and different geometries. Preferably, a complete measurement of geometry over the entire tube length has to be done before each experiment. Additionally, the movement of the tube has to be restricted in the radial direction before and after the die. The

movement of the plug should be recorded during the drawing process.

A clear correlation between dimensional irregularities and stresses cannot be observed in the investigated tube, though there is good agreement with the FEM. With the knowledge of real tube geometry and the additional boundary condition, the results of the simulation should

then show even better agreement. However, compared to FEM calculations, the level of the residual stresses calculated by measured strains is lower. Aging effects can be a reason for this difference. It had been observed that the tensile strength of copper can decrease by more than 40 pct already within the first 10 days after deformation.[19] Then the decrease continues only slowly. Taking into account that the samples were measured 1 year after fabrication and because the trend of measured data corresponds to the calculations, we can state a satisfactory agreement between the model and measurement. More investigations will be performed to clarify this situation.

ACKNOWLEDGMENTS

REFERENCES

1. M. Jansson, L. Nilsson, and K. Simonsson: *J. Mater. Proc. Technol.*, 2007, vol. 190, pp. 1–11.
2. "Seamless Precision Steel Tubes for Hydraulic Cylinders," Report No. TN 008–00, Tenaris Industrial and Automotive Service, 2003, http://www.tenaris.com/shared/documents/files/CB34.pdf.
3. Cole and Swallow: Information on http://www.coleandswallow.com (available in Mar. 2008).
4. *Specialty Steels Product Reference Manual*, Atlas Steel Products Co., Twinsburg, OH, 2000.
5. Tectube Product Specification TI–001, KM Europa Metal AG, Osnabrück, Germany, 2003, www.kme.com/de/service/broschueren.
6. K. Laue and H. Stenger: *Strangpressen*, Aluminium–Verlag Dusseldorf, 1976, ISBN 3-87017-103-0.
7. R. Todd, D. Allen, and L. Alting: *Manufacturing Processes Reference Guide*, Industrial Press Inc., 1994, ISBN 0-8311-3049-0.
8. H.-J. Gummert: Ziehen - über die Herstellung von Drähten, Stangen und Rohren, F&S Druck GmbH, Oldenburg, 2005, ISBN 3-00-016406-5.
9. J. Gebhardt: Werkstoffuntersuchungen zum Ziehen von Rohren mit und ohne Innenwerkzeug, Dr.-Ing. Dissertation, Clausthal University of Technology, Clausthal-Zellerfeld, Germany, 1984.
10. H.-J.Gummert: Ein Beitrag zur Untersuchung des Umformverhaltens von exzentrischen Rohren beim Kaltgleitziehen, Dr.-Ing. Dissertation, Clausthal University of Technology, Clausthal-Zellerfeld, Germany, 1991.
11. E. Macherauch, H. Wohlfahrt, and U. Wolfstieg: *Härtereitechnische. Mitteilungen.*, 1973, vol. 28, p. 201.
12. A. Carradò, D. Duriez, L. Barrallier, S. Brück, A. Fabre, U. Stuhr, T. Pirling, V. Klosek, and H. Palkowski: *Mater. Sci. Forum*, 2008, vol. 21, pp. 571–72.
13. H. Palkowski: Proposal for project AIF 13939, IMET, TU Clausthal, Clausthal-Zellerfeld, Germany, 2003.
14. R.I. Stephens, A. Fatemi, R.R. Stephens, and H.O. Fuchs: *Metal Fatigue in Engineering*, 2nd ed., Wiley-Interscience, John Wiley & Sons, Inc., New York, 2001, ISBN 0-471-51059-9.
15. C. Genzel, W. Reimers, R. Malek, and K. Pöhlandt: *Mater. Sci. Eng.*, 1996, vol. A205, pp. 79–90.
16. H. Palkowski and S. Brueck: Einfluss der Fertigungsparameter auf die Eigenspannungen und Maßtoleranzen beim Rohrziehen, Intermediate Report to Project AIF 13939, IMET, TU Clausthal, Clausthal-Zellerfeld, Germany, 2006.
17. P.J. Boucharda, D. George, J.R. Santisteban, G. Bruno, M. Dutta, L. Edwards, E. Kingston, and D.J. Smith: *J. Pressure Vessel Technol.*, 2005, vol. 82, pp. 299–310.
18. T. Pirling, G. Bruno, and P.J. Withers: *SALSA, Advances in Residual Stress Measurement at ILL Materials Science Forum*, Trans Tech Publications Inc., Switzerland, 2006, vols. 524–525, pp. 217–22, ISSN: 0255-5476.
19. K. Stork: Vergleich des Umformverhaltens verschiedener kontinuierlich vergossener Kupferdrähte, Dr.-Ing. Dissertation, Clausthal University of Technology, Clausthal-Zellerfeld, Germany, 1998.
20. P.J. Dreher: *Metall*, 1970, vol. 10, pp. 1068–73, ISSN 0026-0746.
21. W. Dahl and H. Mühlenweg: *Stahl u. Eisen*, 1964, vol. 84, pp. 1250–60, ISSN 0340-4803.
22. H. Bühler and P.-J. Kreher: *Archiv für das Eisenhüttenwesen*, 1968, pp. 353–59, ISSN 0003-8962.
23. H. Palkowski and S. Brück: *Metall*, 2007, vol. 11, pp. 708–13, ISSN 0026-0746.
24. P. Funke: Collection of flow curves, internal document, Clausthal University of Technology, until 1995.